Fat water separation and field map estimation with multiresolution region growing algorithm

Chuanli Cheng[1,2], Chao Zou[1], Hairong Zheng[1], and Xin Liu[1]

[1]*Paul C. Lauterbur Biomedical Imaging Research Center, Shenzhen Institutes of Advanced Technology, Chinese Academy of Sciences, Shenzhen, Guangdong, China,*

[2]*University of Chinese Academy of Sciences, Beijing, Beijing, China*

Introduction: Fat water separation technique has many MRI clinical applications such as fat suppression in large field inhomogeneity and fat quantification. Traditional methods for fat water separation relied on voxel-wise iterative fitting based on multi-echo data [1]. However, fat water swap due to the large field inhomogeneity or ambiguity in pixel with only one component becomes problematic. Several methods have been proposed to address this problem, such as region growing [2] and multiresolution method [3]. Although these methods have been applied successfully to many cases, there still exist challenges with multiple disjoint regions or drastic change of B_0. In this paper, a novel multiresolution region growing algorithm is introduced for robust fat water separation and accurate field map estimation from three-point non-equally spaced multi-echo images.

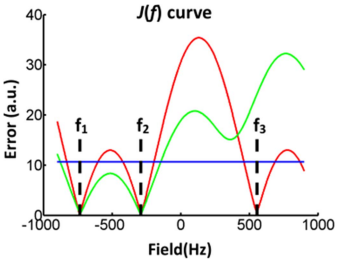

Figure 1: $J(f)$ curves of equally spaced TEs (red) and non-equally spaced TEs (green). With threshold (blue), the false minimum at 555Hz is excluded.

Theory: Our method has two main features: non-equally spaced TEs and multiresolution region growing scheme. First, by using the non-equally spaced TEs, the number of false local minima can be decreased with a proper threshold in error-field curve $\boldsymbol{J}(f)$ defined by Lu et al [4]. As shown in Figure 1, the $\boldsymbol{J}(f)$ curves of equally spaced TEs (5.60/6.38/7.15ms) and non-equally spaced TEs (5.60/6.85/7.15ms) for pixel with water fat ratio = 1:100 and f = -289 Hz are shown. With a proper threshold, the false value at 555Hz can be excluded for non-equally spaced TEs. Second, different from previous algorithms, the region growing is done independently in each resolution, as shown in Figure 2. For each resolution, the image is partitioned into sub-regions with corresponding size. For the sub-region $\boldsymbol{R}$, all local minima of $\boldsymbol{J}_d(f) = \sum_{r\in R}\boldsymbol{J}(r,f)$ are found and saved in set $\boldsymbol{F}$. The seed sub-regions in each resolution are selected according to two criteria: the SNR of the sub-region is large enough, and only one local minimum after thresholding occurs in the $\boldsymbol{J}_d(f)$ curve in the given field range. Figure 3 shows the $\boldsymbol{J}_d(f)$ curve of a seed sub-region in a c-spine data (red square area in Figure 2). After seed sub-regions are chosen, the region growing algorithm is executed among the sub-regions. The grown field maps are used as initial values for accurate search for field map value for each pixel within the sub-region. The obtained field maps of seed sub-regions from all resolutions are combined together. In the finest resolution the whole image is grown from the combined field map.

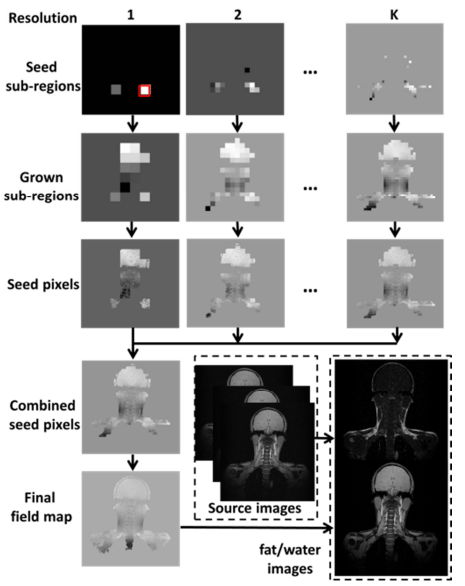

Figure 2: Flow chart of multiresolution region growing

Materials and Methods: The proposed method was tested on c-spine and ankle data. Three volunteers with informed consent (IRB approved) were recruited. The MRI scan in c-spine/ankle was implemented on a 3T system (TIM TRIO, Siemens, Germany) with a FLASH sequence. The basic protocols for the study were: TR = 40ms (c-spine)/25ms (ankle), matrix = 320×320 (c-spine)/ 256×176 (ankle), slice thickness = 3mm, flip angle = 15° (c-spine)/10° (ankle), TE = 5.60/6.85/7.15ms.

The algorithm was implemented in MATALB (Mathworks, NATICK, USA). For the multiresolution scheme, the sub-region in coarsest resolution contained 64×64 pixels, and the zoom factor was 2. The fit error for each sub-regions were evaluated in field range [-900, 900] Hz with step of 3 Hz. For the region growing scheme, sub-regions with more seed sub-regions in the 8-neiborhood had higher priority to be grown. The field value was chosen out from the field value set $\boldsymbol{F}$ by minimizing the field change between seed sub-regions and current sub-region. In the final field map combination step, pixels with large field inconsistency from different resolutions were excluded from seed pixels.

Results: In all studies, fat/water images and field maps were successfully derived from three-point non-equally spaced images. Figure 4(a-b) shows the separated fat/water images and the field maps of a sagittal and a coronal slice of c-spine. Figure 4(c) shows a sagittal slice of ankle. The results show that the algorithm works well with the disjoint area (such as chin) and fast varying field area in the neck and ankle.

Discussions: Although the non-equally spaced TEs scheme is suboptimal in NSA, it decreases the number of false local minima and probability of fat water swap. Different from multiple seed region growing method [2], our method finds seed regions in multiple resolutions, and the seed regions found by our method is much larger since our method is capable of finding the area containing both fat and water with smooth field distribution. Different from other multiresolution methods [3, 4], the field estimation is done independently in each resolution in our method, while field estimation is highly correlated between resolutions in these multiresolution methods. The independent field estimation in each resolution avoids the premature convergence in field search due to drastic changes of B_0 in the finer resolution. Besides, true field map rather than phasor can be estimated from our method.

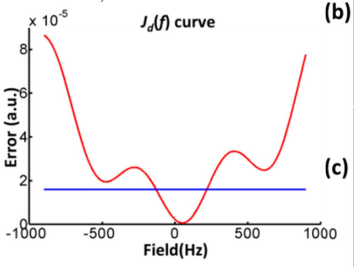

Figure 3: $J_d(f)$ curve (red) of the seed sub-region with red square in Figure 2. With the threshold (blue), only one local minimum is preserved.

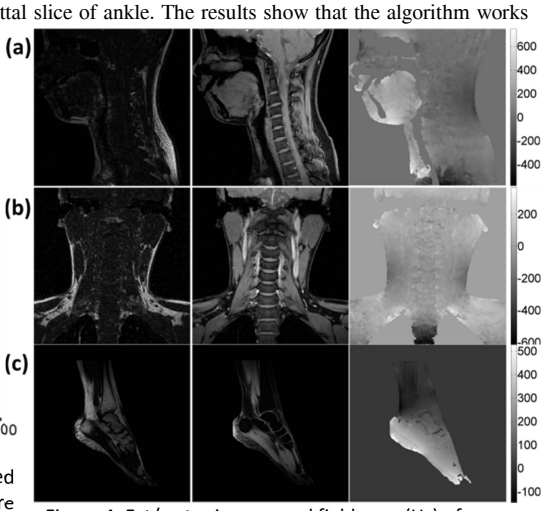

Figure 4: Fat/water images and field map (Hz) of: (a) sagittal slice of c-spine; (b) coronal slice of c-spine; (c) sagittal slice of ankle.

Conclusions: A novel multiresolution region growing algorithm for fat water separation with field map estimation is proposed. The volunteer studies on c-spine and ankle show that the method is robust in large field inhomogeneity and disjoint areas.

Reference: 1. Reeder et al., MRM 2004, 51:35-45; 2. Berglund et al., MRM 2010, 63:1659-1668; 3. Tsao et al., MRM 2013, 70:155-159; 4. Lu et al., MRM 2008 60:236-244.